Propagation Analysis of 6G Millimeter-Wave Communication in Tropical Urban Environments Using NYUSIM

Ami Lia Rizki, Yunida Yunida, Syahrial Syahrial, and Nasaruddin Nasaruddin *

Department of Electrical and Computer Engineering, Faculty of Engineering, Universitas Syiah Kuala, Banda Aceh, Indonesia

Email: ami.lia@mhs.usk.ac.id (A.L.R.); yunida@usk.ac.id (Y.Y.); syahrial@usk.ac.id (S.S.); nasaruddin@usk.ac.id (N.N.)

*Corresponding author

***Abstract*—Mobile communication technology is evolving toward the Sixth Generation (6G), which is designed to deliver ultra-high data rates and support advanced applications including the Internet of Everything (IoE), virtual reality, and artificial intelligence. Realizing such performance demands millimeter-wave (mmWave) and early sub-terahertz frequencies; these bands offer broad bandwidth yet are vulnerable to propagation impairments, especially in tropical environments. Taking Banda Aceh, Indonesia as a tropical urban case, this paper investigates the propagation characteristics of 6G mmWave signals at 28, 38, 73, and 142 GHz. Simulations are built upon the 3rd Generation Partnership Project Technical Report 38.901 (3GPP TR 38.901) channel model integrated within the NYUSIM simulator, with standard Line-of-Sight (LOS) and Non-Line-of-Sight (NLOS) propagation scenarios configured. To faithfully replicate tropical atmospheric conditions, local meteorological parameters (temperature, humidity, air pressure, and rainfall) are imported into baseline simulation outputs via an external attenuation model. This work evaluates core channel metrics: path loss, received power, and Root Mean Square (RMS) delay spread, and compares baseline and climate-aware simulation cases to quantify atmospheric attenuation impacts. The simulation results reveal that path loss and delay spread rise alongside frequency and transmission distance, while the received power drops considerably at higher frequencies. Climate-induced attenuation exerts a limited influence on low mmWave bands over short distances; however, its effect becomes far more prominent at higher frequencies, particularly at 142 GHz, due to intensified atmospheric absorption. These observations demonstrate the frequency-dependent characteristics of climatic impacts and identify critical deployment obstacles for high-frequency wireless communication systems in tropical cities. This study delivers valuable references for preliminary 6G network planning and deepens the understanding of climate-sensitive propagation in mmWave and early sub-terahertz spectrums.**

***Keywords*—Sixth Generation (6G), millimeter-wave (mmWave), tropical urban environment, propagation, NYUSIM**

I. INTRODUCTION

Cellular communication technology is advancing toward the Sixth Generation (6G), expected to be launched around 2030. As an evolution of 4G and 5G systems, 6G aims to deliver data rates of up to 1–10 Tbps while supporting emerging technologies such as the Internet of Everything (IoE), Virtual Reality (VR), Three-Dimensional (3D) gaming, Artificial Intelligence (AI), and Machine-to-Machine (M2M) communications. These applications demand ultra-high data rates, extremely low latency, and high reliability [1].

Recent studies and regulatory actions by the Federal Communications Commission (FCC) have enabled access to spectrum beyond 95 GHz and up to 3 THz, supporting the development of next-generation wireless systems, including 6G [2]. The World Radio Communication Conference (WRC-23) officially identified the 6.425 GHz–7.125 GHz frequency band for International Mobile Telecommunications (IMT) use in regions 1 and 3, which includes Indonesia [3]. However, the use of the 6.425 GHz–7.125 GHz spectrum is still inadequate to fully support IoT-based smart city applications. Hence, millimeter-wave (mmWave) frequencies have emerged as a promising alternative due to their ability to provide significantly higher throughput, despite their limited propagation range.

Research on mmWave communication systems in Indonesia mainly focuses on 5G. Previous research has analyzed the impact of tropical rainfall on mmWave link performance and availability, showing significant attenuation variations across Indonesian cities [4], while studies in Bandung have revealed that 28 GHz and 73 GHz frequencies experience severe attenuation and sensitivity to delay [5]. In tropical regions such as Indonesia, several studies have examined the impact of environmental factors on 5G millimeter-wave channel performance. For instance, a study conducted in Palembang at 28 GHz demonstrated

Manuscript received December 14, 2025; revised April 4, 2026; accepted April 16, 2026; published August 12, 2026.

that increased humidity slightly degrades system performance, particularly in terms of outage probability and Bit Error Rate (BER). However, the impact was found to be relatively minor and may be considered negligible for practical applications [6]. However, previous studies have mainly focused on 5G mmWave propagation, and none have comprehensively analyzed 6G frequencies above 100 GHz under Indonesian urban climatic conditions. This highlights a research gap concerning high-frequency mmWave signal propagation for future 6G systems, specifically in tropical environments such as Indonesia.

Therefore, this paper aims to analyze the propagation characteristics of 6G mmWave communication using the 3rd Generation Partnership Project Technical Report 38.901 (3GPP TR 38.901) model in the urban environment of Banda Aceh, extending the frequency range up to 142 GHz to represent the early stages of 6G spectrum exploration. Four frequencies, 28 GHz, 38 GHz, 73 GHz, and 142 GHz, are compared to evaluate their path-loss, received-power, and delay-spread characteristics [7, 8].

The selected carrier frequencies represent different stages in the development of the mmWave and early sub-THz spectrum. The 28 GHz and 38 GHz bands are typically considered suitable frequencies for initial mmWave deployments. In contrast, the 73 GHz band is part of the higher mmWave spectrum currently being explored for future high-capacity systems. The 142 GHz band, which is part of the D-band spectrum, has recently been considered as a potential early sub-THz frequency for 6G communications. By comparing these frequencies, we can analyze propagation behavior across a broad range of spectra relevant to future 6G systems.

In addition, the use of multiple carrier frequencies enables the analysis of how climate-related attenuation varies across different regions of the mmWave and early sub-THz spectrum. Atmospheric absorption, humidity effects, and rain attenuation are known to be frequency-dependent, with higher frequencies generally experiencing stronger attenuation. Therefore, comparing propagation performance across 28 GHz to 142 GHz allows this study to explicitly evaluate how the impact of tropical climate conditions changes with frequency, particularly highlighting the increasing sensitivity of higher-frequency bands to atmospheric effects.

The main contribution of this work is the development of a propagation analysis framework designed to evaluate the performance of millimeter-wave and early sub-terahertz communication systems in tropical urban environments for future 6G applications. Within this framework, we analyze propagation characteristics at frequencies of 28 GHz, 38 GHz, 73 GHz, and 142 GHz using the 3GPP TR 38.901 channel model, as implemented in the NYUSIM simulator. This modeling reflects urban conditions specific to Banda Aceh, Indonesia. To ensure realistic tropical atmospheric conditions, we incorporate representative local climate parameters, including temperature, humidity, air pressure, and rainfall, obtained from the Meteorology, Climatology, and Geophysics Agency (BMKG) data. The analysis evaluates key channel performance metrics, including path loss, received power, and delay spread, under both Line-of-Sight (LOS) and Non-Line-of-Sight (NLOS) scenarios. By examining propagation behavior across multiple frequency bands relevant to future 6G systems, this work provides valuable insights into the feasibility and challenges of deploying high-frequency mmWave and early sub-THz communication systems in tropical urban contexts.

II. Related Works

The evolution of wireless communication technologies from the First Generation (1G) to the Fifth Generation (5G) has demonstrated significant improvements in both network capacity and data transmission speed. The Fifth Generation (5G) has reached throughput rates of up to 1 Gbps, supported by technologies such as Multiple Input Multiple Output (MIMO) and Filter Bank Multicarrier (FBMC). However, it still faces limitations in meeting the growing demands of future applications. Currently, wireless communication technology is advancing toward the Sixth Generation (6G), which is expected to overcome these challenges and further expand network capacity to accommodate increasingly complex requirements.

The 6G system incorporates more sophisticated technologies, including Artificial Intelligence (AI) applications, which distinctly differentiate it from previous generations. Although still in its early stages, 6G is expected to achieve data rates of 1–10 terabits per second (Tbps), positioning it as a key enabler and foundational backbone of future communication infrastructures [9, 10]. In 6G networks, three main communication scenarios are being developed to meet future connectivity demands, as illustrated in Fig. 1.

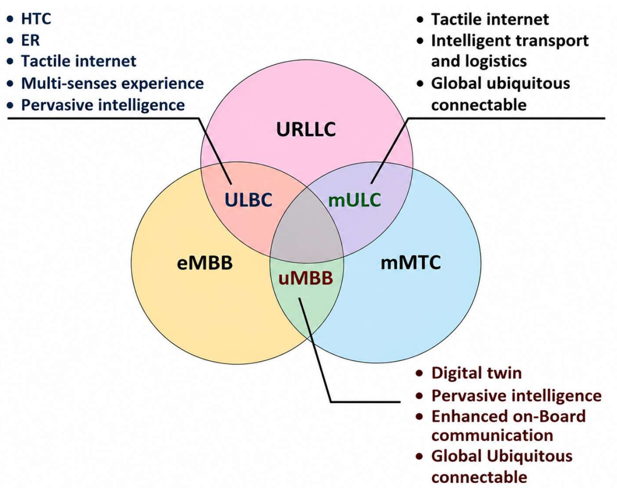

Fig. 1. Scenario 6G [1].

The first scenario, ultra-Mobile Broadband (uMBB), is designed to support global connectivity and high-quality communication services, including digital twins, onboard communication, and universal access across various environments. The second scenario, Ultra-Reliable Low Latency Broadband Communications (ULBC), provides high throughput and extremely low latency, making it ideal for applications such as holographic communication, tactile internet, Extended Reality (XR), and AI-based systems [1].

The third scenario, massive Ultra-Reliable Low Latency Communication (mULC), combines Ultra-Reliable Low Latency Communication (URLLC) and massive Machine Type Communication (mMTC). This scenario enables large-scale deployment of sensors and actuators across various industrial sectors. Collectively, the three new scenarios, uMBB, ULBC, and mULC, extend the previous 5G scenarios (eMBB, URLLC, and mMTC), forming a comprehensive framework for diverse applications and communication requirements in 6G networks [1].

One of the key enablers for realizing 6G is the utilization of the millimeter-wave (mmWave) spectrum. The mmWave frequency band spans from 30 GHz to 300 GHz**,** with wavelengths ranging from 1 to 10 millimeters shorter than microwaves and longer than infrared waves. This range lies between the microwave band (3 GHz –30 GHz) and overlaps with the terahertz frequency range (100 GHz–30 THz) [11]. The mmWave spectrum offers wide bandwidth, compact antenna dimensions, and high capacity, supporting advanced applications such as Virtual Reality (VR), holographic communication, and smart city infrastructure.

A. Recent mmWave Measurements Above 100 GHz

To support the development of next-generation communication systems, recent research efforts have increasingly focused on exploring the D-band (110–170 GHz) and sub-terahertz (sub-THz) frequencies. These studies aim to characterize propagation behavior, evaluate channel parameters, and refine existing channel models beyond the 100 GHz range, which remains underrepresented in standardized frameworks such as 3GPP TR 38.901. Ju and Rappaport [11] conducted wideband channel measurements at 142 GHz in indoor factory environments to develop a statistical channel model for sub-THz industrial wireless networks. Their results indicated that path loss increases logarithmically with frequency, and that the delay spread at 142 GHz strongly depends on the Line-of-Sight (LOS) condition and on the reflection properties of metallic surfaces. Despite the higher attenuation compared to 28 GHz and 73 GHz, reliable short-range communications were still achievable below 100 m, particularly with directional antenna alignment and minimal obstructions. This study provides one of the first comprehensive channel models in the D-band, demonstrating its applicability to future 6G industrial and indoor scenarios.

Complementing this work, Bian *et al.* [12] conducted outdoor channel measurements across the D-band (110 GHz–170 GHz) to investigate long-distance propagation up to 800 m. Their findings revealed that path-loss exponents increase with frequency, indicating greater attenuation at higher D-band frequencies, particularly under NLOS conditions. However, the use of high-gain directional antennas effectively mitigated signal degradation, enabling multi-gigabit-per-second data rates over moderate distances.

Collectively, these studies demonstrate that mmWave and sub-THz frequencies above 100 GHz hold strong potential for high-capacity 6G systems. Nonetheless, most existing measurement campaigns have been conducted in temperate regions, leaving a limited understanding of propagation behavior in tropical environments such as Indonesia. This research gap highlights the necessity of extending current models (e.g., 3GPP TR 38.901) to account for humidity, temperature, and rainfall, ensuring more accurate channel predictions and robust network design for future 6G deployments in tropical regions.

B. Previous Studies on mmWave Propagation

To provide a comprehensive overview of previous research on mmWave communication, Table I summarizes key studies, their frequency ranges, channel models, scenarios, and main findings. This includes studies conducted in Indonesia on 5G mmWave propagation [4−6] and recent research on D-band and sub-THz measurements [11, 12].

TABLE I. SUMMARY OF PREVIOUS MMWAVE PROPAGATION STUDIES

Ref.	Frequency (GHz)	Model	Scenario	Key Findings
[4]	N/A	Measurement	Urban	Significant attenuation due to tropical rainfall
[5]	28, 73, 4	NYUSIM	5G Urban (UMi and UMa)	High attenuation delay sensitivity
[6]	28	NYUSIM	5G Urban Micro	Air pressure, temperature, and rain rate
[11]	142	Statistical CH Model	Indoor Factory	High path loss
[12]	110–170	Measurement	Outdoor D-Band	High path loss; NLOS losses
This paper	28–142	3GPP TR 38.901	6G Urban	High path loss, higher delay spread, NLOS losses

III. SYSTEM AND CHANNEL MODEL

This section outlines the assumptions regarding signal propagation, the analytical formulations used, and the simulation parameters adopted to assess the behavior of millimeter-wave (mmWave) and early sub-terahertz (sub-THz) channels in tropical urban environments. The models utilized are based on the 3GPP TR 38.901 framework as implemented in NYUSIM, with additional climate-specific attenuation adjustments applied during post-processing.

Fig. 2 illustrates the workflow of the research methodology used in this study. The process begins with a literature review to identify the relevant theoretical background and research gaps related to mmWave and 6G propagation. Next, the study area is identified, focusing on the urban environment of Banda Aceh. Climate data, including temperature, humidity, air pressure, and rainfall, are then obtained from the Indonesian Agency for Meteorology, Climatology and Geophysics (BMKG) meteorological database to represent local atmospheric conditions.

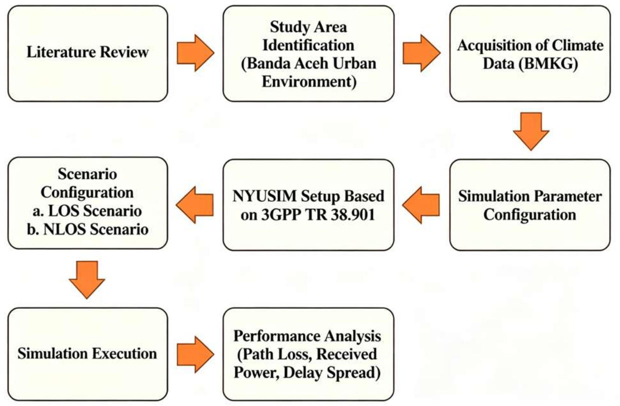

Fig. 2. Research workflow for configuring the NYUSIM simulator based on the 3GPP TR 38.901 channel model and evaluating LOS and NLOS propagation scenarios.

Subsequently, the simulation parameters are configured, including carrier frequency, bandwidth, transmit power, antenna height, and propagation distance. The NYUSIM simulator is then configured based on the 3GPP TR 38.901 channel model. The propagation conditions are modeled using the standard LOS and NLOS scenarios available in NYUSIM, representing typical urban propagation environments. After the simulation setup is completed, simulations are executed to generate channel data. Finally, the simulation outputs are analyzed by evaluating key performance metrics, including path loss, received power, and delay spread.

A. Radio Wave Propagation Scenarios and Performance Parameters

This section explores the two primary scenarios of radio wave propagation, i.e., LOS and NLOS, as depicted in Fig. 3. LOS propagation refers to the electromagnetic radiation characteristic in which two stations can transmit and receive signals without obstruction between their transmitting and receiving antennas. Although the transmission path appears unobstructed, phenomena such as reflection and scattering from nearby small objects may still occur [13].

Fig. 3. Radio wave propagation scenarios.

In 6G mmWave technology, LOS propagation plays a crucial role as it provides better transmission performance with relatively low signal attenuation. Conversely, NLOS propagation occurs when there is no direct line of sight between the transmitter and receiver due to physical obstacles, such as trees or dense structures. In this condition, the signal reaches the receiver through indirect paths, which introduces additional attenuation and signal degradation. This phenomenon poses a major challenge for high-frequency wireless communication systems such as mmWave, as the shorter wavelength makes the signal more susceptible to blockage by environmental objects [14].

1) Path loss

Path loss refers to the phenomenon of signal power attenuation as it propagates from the transmitting antenna to the receiving antenna through the transmission medium. In this study, the Close-In (CI) free space reference distance is employed to estimate path loss, which is expressed as follows [15]:

$$PL^{CI}(f,d)[\text{dB}] = FSPL(f,1\,\text{m})[\text{dB}] + 10\eta\log_{10} d + AT[\text{dB}] + O2I[\text{dB}] + FL[\text{dB}] + X_{\sigma}^{CI} \quad (1)$$

where f is the operating frequency in Gigahertz (GHz), d is the distance between the transmitter and receiver in meters (m), and η is the path-loss exponent that describes the rate of signal attenuation with increasing distance. The term AT represents atmospheric attenuation, $O2I$ denotes outdoor-to-indoor penetration loss, and FL represents additional attenuation caused by foliage, such as trees and leaves. Furthermore, X_{σ}^{CI} represents the large-scale shadow-fading component, which is commonly modeled as a zero-mean Gaussian random variable with a standard deviation of σ dB.

The Free Space Path Loss (FSPL) at a reference distance of 1 meter is calculated as:

$$FSPL(f,1\,\text{m})\,[\text{dB}] = 20\log_{10}\left(\frac{4\pi f \times 10^9}{c}\right) = 32.4\,\text{dB} + 20\log_{10}(f) \quad (2)$$

where f is the operating frequency in Gigahertz (GHz), and c is the speed of light in a vacuum, approximately 3×10^8 m/s.

AT[dB] indicates the extra attenuation caused by environmental factors such as rain, fog, buildings, vegetation, or air particles. The standard 3GPP TR 38.901 channel model does not explicitly account for climate variables. To address this, we incorporated climate parameters by adjusting the atmospheric attenuation term in the path loss calculation. We estimated the atmospheric attenuation coefficient based on local meteorological conditions, including temperature, humidity, air pressure, and rainfall, using data from BMKG. The additional attenuation component was then calculated as follows:

$$AT[dB] = \alpha\,[dB/m] \times d\,[m] \quad (3)$$

where α represents the atmospheric attenuation coefficient (dB/m), and d denotes the propagation distance. This attenuation term was added to the conventional CI path-loss model used in NYUSIM simulations to account for the effects of tropical atmospheric conditions.

Finally, X_σ^{CI} is a Gaussian random variable with a mean of 0 and a standard deviation in dB, representing shadow fading random fluctuations in path loss due to large obstructions (e.g., tall buildings or dense vegetation) that cause deviations from the average path loss value [16]. In this study, the atmospheric and rain attenuation term AT is not generated internally by NYUSIM. Instead, AT is calculated externally based on the local climate parameters of Banda Aceh and then added as an additional loss component to the path loss obtained from NYUSIM. This approach allows the impact of tropical temperature, humidity, air pressure, and rainfall to be evaluated without modifying the internal channel generation procedure of the simulator.

2) Received power

The received power level represents the amount of signal power transmitted from the transmitter and successfully received by the receiver. This value reflects the minimum signal power threshold required to maintain optimal communication performance [17]. Mathematically, the received power (P_r) can be expressed using the following propagation analysis equation.

$$P_r(d)(dBW) = P_t(dBW) + G_t + G_r - PL^{CI}(f,d)(dB) \quad (4)$$

where P_t denotes the transmit power in decibel-watts dBW, G_t and G_r represent the transmitter and receiver antenna gains in decibel-isotropic (dBi). $PL^{CI}(f,d)$ corresponds to the path loss at frequency f and distance d, based on a reference distance of 1 meter, considering both LOS and NLOS propagation conditions under the Urban Microcell (UMi) scenario. For omnidirectional antennas, G_t and G_r are typically 0 dBi, whereas for directional antennas, both gains are computed from the effective aperture corresponding to the operating frequency. In this study, the path loss obtained from NYUSIM does not include additional attenuation components such as atmospheric and rain losses, building penetration loss ($O2I$), Foliage Loss (FL), or shadow fading (X_σ^{CI}). The atmospheric and rain attenuation are subsequently introduced as an external loss component based on local climate data [18].

3) Delay spread

Delay spread is a measure of the temporal dispersion of multipath signals in a wireless channel, representing the difference between the earliest- and latest-arriving signal components. In general, delay spread indicates the level of temporal spreading in the propagation environment. A larger delay spread increases the likelihood of Inter-Symbol Interference (ISI), which can lead to signal distortion and overall degradation of communication quality. In recent studies, delay spread is commonly quantified using the Root Mean Square Delay Spread (RMS-DS), which characterizes the distribution of multipath energy over time. RMS-DS has been widely applied in mmWave and sub-THz channel research to analyze multipath characteristics across various propagation scenarios [19].

In this study, both LOS and NLOS scenarios are generated using the standard UMi scenario defined in 3GPP TR 38.901 and implemented in NYUSIM, with identical simulation settings except for the presence of direct visibility between the transmitter and receiver.

B. Study Area and Simulation Setup

The research was conducted in Banda Aceh City using two propagation conditions as depicted in Fig. 4 and Fig. 5. The LOS condition utilized the Blang Padang Field, which provides a clear and open area with a direct transmitter–receiver line and minimal physical obstructions. This environment allows evaluation of pure LOS characteristics with low scattering effects. Meanwhile, the NLOS condition was modeled in the RSUDZA Hospital area, which features multiple closely spaced buildings that block the direct path. This setting represents a typical urban NLOS environment where signal propagation is dominated by reflection, diffraction, and scattering, making it suitable for analyzing mmWave behavior under obstructed conditions.

Fig. 4. LOS area with clear transmitter-receiver visibility at Blang Padang Field, Banda Aceh.

Fig. 5. NLOS area around RSUDZA Hospital with buildings obstructing the signal path.

1) Climate data and channel parameters

The climate data were obtained from the BMKG (Meteorological, Climatological, and Geophysical

Agency), Class IV Aceh Climatology Station, for the year 2023. The recorded average temperature was 27.41 °C, with 77.89% humidity, 1007.83 mbar air pressure, and a rainfall rate of 0.293 mm/hr [20]. The channel parameters used in the simulation are presented in Table II.

TABLE II. CHANNEL PARAMETER

No	Parameter	Value	
1	Frequency	28 GHz, 38 GHz, 73 GHz, and 142 GHz [7, 8]	
2	Bandwidth	800 MHz	28 GHz, 38 GHz, 73 GHz
		1000 MHz	142 GHz
3	Transmit Power	30 dBm	
4	Scenario	Umi	
5	Distance	50–100 m [21]	
6	Antenna Height	10 m [21]	
7	UE Height	1.5 m [21]	
8	Radiation Pattern	Omnidirectional	
9	Propagation Conditions	LOS and NLOS	

The transmit power of 30 dBm was chosen to represent a typical configuration for small-cell base stations in mmWave systems. The bandwidths of 800 MHz and 1000 MHz correspond to commonly allocated wideband channels within the mmWave frequency range for 5G and future 6G systems. The Urban Micro (UMi) scenario is chosen because Banda Aceh's urban area shares similar physical characteristics, including moderate building density and microcell coverage. The distance range of 50–100 m reflects realistic operational ranges of mmWave cells due to their limited coverage. Omnidirectional antennas are used as a baseline evaluation, allowing channel characteristics to be observed without directional beamforming influence. Although practical mmWave and sub-THz systems rely heavily on directional antennas and beamforming, the omnidirectional assumption in this study is intentionally adopted to isolate the effects of propagation and climate-related attenuation and to enable fair comparison across different frequencies and scenarios.

The specific atmospheric and rain attenuation coefficient, α (dB/m), is calculated based on standard atmospheric and precipitation attenuation models that consider local temperature, relative humidity, air pressure, and rainfall rate obtained from BMKG [20]. The total additional attenuation is then computed as $AT = \alpha \cdot d$ and is added to the path loss generated by NYUSIM in a post-processing step. In this work, the LOS and NLOS channel realizations are first generated using the standard 3GPP TR 38.901 model implemented in NYUSIM. Subsequently, the climate-dependent attenuation term is applied equally to both LOS and NLOS links to quantify the impact of tropical atmospheric and rainfall conditions.

2) *Propagation model design*

The propagation model in this study was analytically validated by ensuring that the path loss formulation, environmental parameters, and UMi scenario settings strictly adhere to the specifications of 3GPP TR 38.901 [21]. Since the research is simulation-based, no field measurements were conducted; instead, model validity was ensured through conformity with the standard. In addition, the expected path loss trends were cross-checked with previous studies at 28 GHz, 38 GHz, 73 GHz, and 142 GHz to confirm the reliability of the modeled propagation characteristics [7, 8]. Additionally, climate-related attenuation is included as an external post-processing loss term, which is applied to the received power and path loss results generated by NYUSIM.

a) *LOS propagation model*

Fig. 6 illustrates the propagation modeling under Line of Sight (LOS) conditions for the Urban Micro (UMi) scenario. The UMi scenario is selected based on the characteristics of Banda Aceh City, which has a dense population and urban environment. The simulation adjusts the distance between the transmitter and receiver from 50 m to 100 m, in intervals of 10 m.

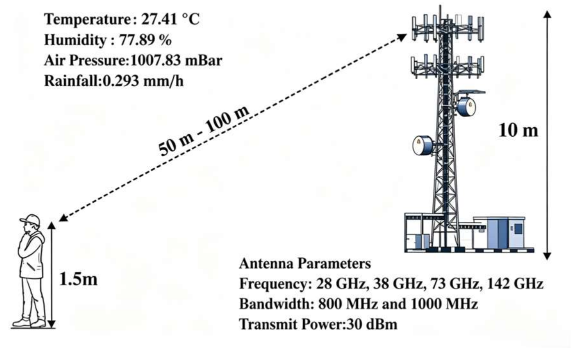

Fig. 6. Configured LOS propagation scenario in NYUSIM under UMi conditions.

b) *NLOS propagation model*

Fig. 7 presents the propagation modeling under Non-Line of Sight (NLOS) conditions for the Urban Micro (UMi) scenario, which is also relevant to the geographical and population density characteristics of Banda Aceh City. The simulation utilizes the same distance variations as in the LOS condition, which range from 50 m to 100 m, with intervals of 10 m.

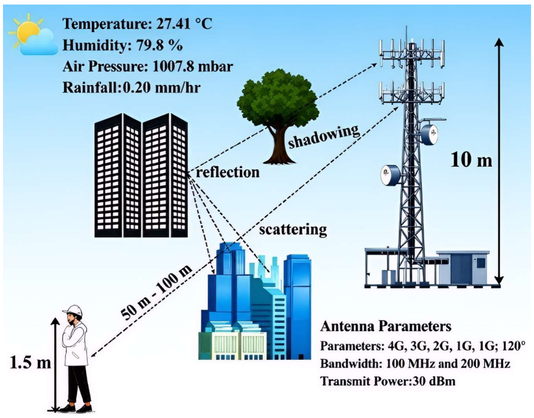

Fig. 7. Configured NLOS propagation scenario in NYUSIM under UMi conditions.

Since neither the 3GPP TR 38.901 channel model nor the NYUSIM simulator explicitly includes climate-dependent atmospheric effects, the local climate parameters are incorporated through an external attenuation procedure applied after channel generation. First, baseline path loss values are generated for both Line of Sight (LOS) and Non-Line of Sight (NLOS) conditions using the NYUSIM model, in accordance with the CI-based path loss standard. Next, representative local meteorological parameters, such as temperature, humidity, air pressure, and rainfall, obtained from the BMKG, are used to estimate the atmospheric attenuation coefficient, denoted as α (dB/m). This estimation considers both standard atmospheric absorption and factors related to rain attenuation.

Based on standard atmospheric attenuation trends under tropical sea-level conditions, the specific attenuation coefficient α was approximated as 0.12, 0.18, 0.45, and 1.80 dB/km for 28 GHz, 38 GHz, 73 GHz, and 142 GHz, respectively. These values include gaseous absorption and humidity-related attenuation under Banda Aceh climate conditions, as shown in Table III.

TABLE III. THE ATMOSPHERIC ATTENUATION COEFFICIENT FOR 28, 38, 73, AND 142 GHZ

Frequency	α gas + humidity (dB/km)	α in (dB/m)
28 GHz	0.12	0.00012
38 GHz	0.18	0.00018
73 GHz	0.45	0.00045
142 GHz	1.80	0.00180

3) Performance simulation setup

This study is primarily based on system-level simulations using the NYUSIM simulator and the standardized 3GPP TR 38.901 channel model, which has been widely validated in previous mmWave propagation studies. While measurement-based validation is important, simulation enables controlled evaluation of propagation behavior across various frequency bands and environmental conditions. This is particularly crucial for early-stage 6G research, where measurement campaigns at sub-THz frequencies are still limited.

In addition, omnidirectional antennas are adopted in this study as a baseline assumption to isolate the fundamental effects of propagation and climate-related attenuation. This approach enables consistent comparison across different frequencies and propagation scenarios without the influence of beamforming gain or antenna directivity. Although practical mmWave and 6G systems rely heavily on directional antennas and beamforming techniques, the current analysis is intended to provide a reference propagation characterization under standardized conditions. Future work will extend this study by incorporating directional antenna models, beamforming gains, and measurement-based validation in real tropical urban environments.

To clearly evaluate the impact of climate parameters on mmWave propagation, two simulation cases are considered in this study: (i) a baseline scenario using the standard NYUSIM output without additional atmospheric attenuation, and (ii) a climate-aware scenario where the atmospheric attenuation term derived from local meteorological data is incorporated. The comparison between these two cases enables a quantitative assessment of the additional loss introduced by tropical environmental conditions across different frequency bands.

IV. RESULTS AND DISCUSSION

To assess the importance of climate-aware attenuation, we analyze all reported propagation trends in relation to the baseline outputs from the NYUSIM simulator. This approach helps us identify the additional loss contributed by local atmospheric conditions across the various frequency bands examined. This section presents simulation results from the NYUSIM simulator for key parameters, including path loss, received power, and delay spread. These results are used to evaluate the performance of the 6G mmWave communication system, as discussed in Section III. The simulations were carried out using the NYUSIM software, which is based on the 3GPP TR 38.901 channel model designed for urban environments. The transmission distance was varied from 50 m to 100 m under both Line-of-Sight (LOS) and Non-Line-of-Sight (NLOS) propagation conditions for frequencies of 28 GHz, 38 GHz, 73 GHz, and 142 GHz. The performance of the system was evaluated to determine the values of path loss, received power, and delay spread in the 6G mmWave network.

It should be noted that the 3GPP TR 38.901 channel model was originally specified and validated for carrier frequencies up to 100 GHz. In this study, the 142 GHz band was included as an exploratory extension to investigate sub-THz propagation characteristics relevant to early-stage 6G research. Although NYUSIM supports simulations at frequencies above 100 GHz, extrapolation of path loss behavior and channel statistics beyond the validated frequency range may introduce modeling uncertainty. Therefore, the results obtained at 142 GHz should be interpreted as indicative propagation trends rather than fully validated predictions, and future measurement-based studies are required to verify model reliability in the sub-THz regime.

A. Path Loss

Under LOS conditions, the lowest path loss was observed at a frequency of 28 GHz, measuring 93.9 dB at a distance of 50 m. In contrast, the highest path loss was observed at 142 GHz and reached 117.5 dB at a distance of 100 m. These results indicate that as the frequency increases, the signal attenuation also becomes more significant. The increase in path loss is primarily caused by higher electromagnetic wave attenuation at higher frequencies and the more dominant atmospheric absorption effects within the mmWave spectrum.

In contrast, under NLOS conditions, signal attenuation increases compared to LOS. At 28 GHz, the path loss rises from 110.7 dB at 50 m to 125.2 dB at 100 m. Meanwhile, at 142 GHz, the path loss reaches 119.1 dB at 50 m and increases to 144.9 dB at 100 m. The difference between LOS and NLOS conditions highlights the significant impact of physical obstructions such as buildings, trees, and reflective surfaces in urban environments, which contribute to higher signal attenuation, particularly at higher frequencies characterized by very short wavelengths.

Fig. 8 shows path loss as a function of transmitter–receiver distance at frequencies of 28, 38, 73, and 142 GHz, under both LOS and NLOS conditions in a tropical urban scenario. It is evident that path loss increases logarithmically with distance and is directly proportional to the operating frequency. Moreover, the gap between LOS and NLOS conditions widens as the propagation distance grows, emphasizing the susceptibility of mmWave signals to environmental factors. These observations are consistent with previous studies, such as Rappaport *et al.* [8], which reported that urban mmWave channels exhibit higher attenuation at frequencies above 28 GHz, particularly in NLOS scenarios. Similarly, Xing and Rappaport [7] found that path loss in NLOS urban environments at 73 GHz can exceed LOS measurements by 15–20 dB over comparable distances. Such comparative results confirm that mmWave communication systems, especially those operating above 70 GHz, require careful link planning and potentially the deployment of beamforming techniques to mitigate signal degradation caused by obstructions.

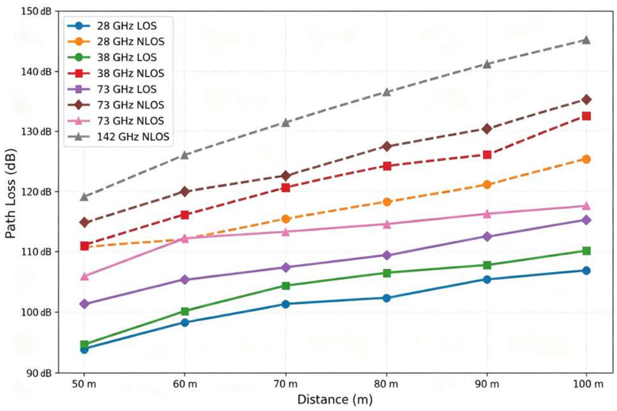

Fig. 8. Path loss as a function of transmitter–receiver distance (m) for carrier frequencies of 28, 38, 73, and 142 GHz under LOS and NLOS conditions in a tropical urban environment.

TABLE IV. LOS COMPARISON (100 M)

Frequency	Baseline Path Loss (dB)	Climate-aware Path Loss (dB)
28 GHz	107.7	107.712
38 GHz	110.3	110.318
73 GHz	114.8	114.845
142 GHz	117.5	117.680

TABLE V. NLOS COMPARISON (100 M)

Frequency	Baseline Path Loss (dB)	Climate-aware Path Loss (dB)
28 GHz	125.2	125.212
38 GHz	129.6	129.618
73 GHz	137.8	137.845
142 GHz	144.9	145.080

The comparison indicates that under short-range urban links (100 m), climate-related attenuation introduces only a minor incremental loss at 28–73 GHz, while the effect becomes more visible at 142 GHz due to stronger atmospheric absorption at higher frequencies. The corresponding comparisons under LOS and NLOS propagation conditions are summarized in Tables IV and V, respectively.

B. *Received Power*

The simulation results are shown in Fig. 9, which compares the received power values against distance for each frequency under both Line of Sight (LOS) and Non-Line of Sight (NLOS) conditions. The simulation clearly demonstrates that the received power decreases consistently as both distance and frequency increase. Under LOS conditions, the highest received power was obtained at 28 GHz, with a value of –63.9 dBm at a distance of 50 m, while the lowest value was recorded at 142 GHz, reaching –87.5 dBm at 100 m. This reduction in received power is mainly due to increased path loss from longer propagation distances and higher atmospheric attenuation at elevated frequencies.

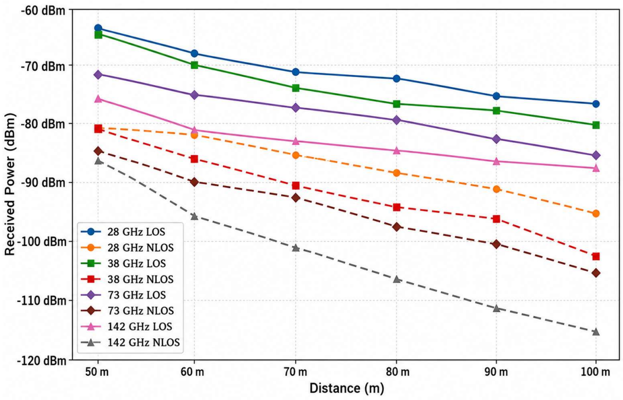

Fig. 9. Received power variation with respect to transmitter–receiver distance (m) for 28, 38, 73, and 142 GHz under LOS and NLOS conditions.

In the NLOS scenario, the reduction in received power is more pronounced compared to the LOS condition. For instance, at 28 GHz, the received power decreases from–80.7 dBm at 50 m to –95.2 dBm at 100 m. Meanwhile, at 142 GHz, it drops from –86.3 dBm to –114.9 dBm over the same distance range. This behavior indicates that in the absence of a direct line-of-sight, the signal undergoes reflections, scattering, and diffraction, which collectively increase total attenuation and degrade the received signal quality.

When comparing across all four frequencies, it can be observed that higher frequencies experience greater reductions in received power, both in LOS and NLOS conditions. For example, at a distance of 100 m, the LOS received power at 28 GHz is –76.7 dBm, whereas at 142 GHz, it reaches –87.5 dBm. This trend highlights that mmWave communication systems operating at higher frequencies are highly dependent on a clear LOS path to maintain optimal signal strength.

Fig. 9 shows the relationship between received power and transmitter-receiver distance for frequencies of 28, 38, 73, and 142 GHz under both LOS and NLOS conditions in a tropical urban scenario. The *x*-axis indicates the transmitter-receiver distance (m), while the *y*-axis represents the received power (dBm). This finding highlights that propagation distance and environmental conditions are the two primary factors affecting the performance of received power in millimeter-wave communication systems. These observations align with earlier millimeter-wave studies. For example, Rappaport *et al.* [8] reported that received power in urban NLOS channels decreases significantly relative to LOS conditions, particularly at frequencies above 28 GHz. Similarly, Xing and Rappaport [7] demonstrated that received power drops substantially at 73 GHz in urban NLOS environments due to dominant multipath effects and atmospheric attenuation. Therefore, the simulation results emphasize the necessity of careful link planning and the potential deployment of mitigation techniques, such as beamforming or base-station densification, to sustain performance in mmWave communication systems, particularly at higher frequencies and under NLOS conditions.

The climate-aware received power results indicate only minor additional degradation at 28–73 GHz within short-range links (100 m), whereas the attenuation becomes more visible at 142 GHz due to stronger atmospheric absorption at higher frequencies. Even under tropical humidity conditions, the incremental received power reduction remains below 0.2 dB over 100 m, indicating that baseline geometric path loss remains the dominant loss mechanism in short urban links. Because the propagation distance is limited to 100 m, the climate-induced attenuation remains relatively small compared with geometric path loss. A detailed comparison of received power under LOS and NLOS conditions is presented in Tables VI and VII, respectively.

TABLE VI. LOS RECEIVED POWER (100 M)

Frequency	Baseline *Pr* (dBm)	Climate-aware *Pr* (dBm)
28 GHz	−76.7	−76.712
38 GHz	−80.3	−80.318
73 GHz	−84.8	−84.845
142 GHz	−87.5	−87.680

TABLE VII. NLOS RECEIVED POWER (100 M)

Frequency	Baseline *Pr* (dBm)	Climate-aware *Pr* (dBm)
28 GHz	−95.2	−95.212
38 GHz	−99.6	−99.618
73 GHz	−107.8	−107.845
142 GHz	−114.9	−115.080

The comparison clearly indicates that climate-induced attenuation has a relatively minor effect at lower mmWave frequencies (28–73 GHz) over short distances, while its impact becomes more noticeable at higher frequencies, such as 142 GHz, due to increased atmospheric absorption. This demonstrates that, although geometric path loss remains dominant in short-range links, climate effects become increasingly relevant at sub-THz frequencies. Additionally, the multi-frequency analysis confirms that the influence of climate-related attenuation becomes more pronounced at higher frequencies, particularly at 142 GHz, demonstrating the frequency-dependent nature of atmospheric effects in tropical environments.

C. Delay Spread

The simulation results are presented in Fig. 10, which illustrates the relationship between distance and delay spread values for each frequency under both propagation conditions.

Fig. 10 illustrates the relationship between RMS delay spread and transmitter-receiver distance for frequencies of 28, 38, 73, and 142 GHz, in both LOS and NLOS conditions within a tropical urban environment. The *x*-axis represents the distance between the transmitter and receiver (in meters), while the *y*-axis indicates the RMS delay spread (in nanoseconds). The results indicate that delay spread increases with distance for all frequencies. Under LOS conditions, the smallest delay spread occurs at 28 GHz, measuring 13.78 ns at 50 m and increasing to 24.92 ns at 100 m. A similar trend is observed for 38 GHz (18.46 ns to 30.84 ns), 73 GHz (19.04 ns to 32.40 ns), and 142 GHz (20.06 ns to 34.52 ns).

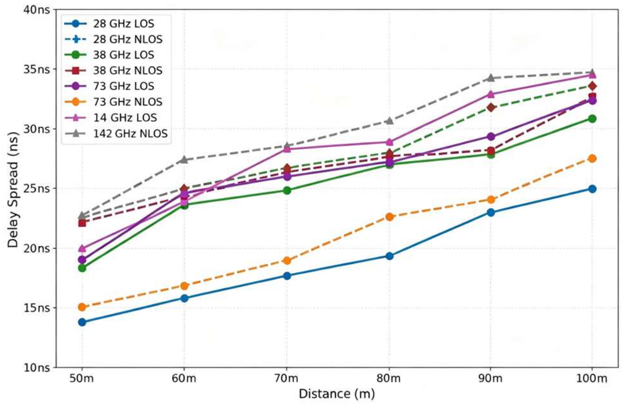

Fig 10. RMS delay spread as a function of transmitter–receiver distance (m) for multiple carrier frequencies under LOS and NLOS conditions.

This increase reflects greater variation in signal arrival times due to the higher number of multipath components at elevated frequencies. Under NLOS conditions, delay spread values are consistently higher than under LOS conditions, reflecting the more complex propagation environment. For instance, at 28 GHz, the delay spread rises from 15.08 ns to 27.44 ns, whereas at 142 GHz, it increases from 22.86 ns to 34.66 ns over the same distance range. This phenomenon is primarily caused by the absence of a direct line of sight, which forces signals to propagate via reflections, scattering, and diffraction, thereby introducing greater variation in arrival times.

The observed trends are in line with previous studies. For example, Rappaport *et al.* [8] reported that urban mmWave NLOS channels exhibit higher delay spreads at frequencies above 28 GHz due to multipath propagation. Similarly, Xing and Rappaport [7] observed that 73 GHz NLOS urban channels exhibit significantly higher delay spreads than LOS scenarios, underscoring the influence of obstructions and environmental complexity on signal dispersion. The increase in delay spread has direct implications for Inter-Symbol Interference (ISI) in high-frequency systems. Hence, 6G mmWave system design must incorporate time-domain compensation and equalization techniques, particularly at frequencies above

70 GHz and over longer transmission distances. Notably, the 142 GHz frequency exhibits the highest delay spread under both LOS and NLOS conditions (34.52 ns and 34.66 ns at 100 m, respectively), highlighting the necessity to account for multipath effects in urban 6G network planning. The results indicate that climate-related attenuation remains limited at lower mmWave frequencies over short urban links but becomes increasingly visible at higher frequencies, particularly near 142 GHz. Although the present study uses standardized simulation assumptions and omnidirectional antennas, the findings provide useful early-stage insight for tropical 6G propagation planning. Future work should include measurement-based validation and directional beamforming analysis.

While the current analysis is based on simulations and assumes omnidirectional antennas, this study aims to provide a baseline climate-aware propagation assessment under standardized urban microcell conditions. Practical 6G deployments will require directional beamforming, adaptive antenna gain, and measurement-based validation, especially at frequencies approaching the sub-THz range. Therefore, the current results should be interpreted as early-stage propagation trends rather than deployment-ready performance predictions.

V. Conclusion

This paper investigates the propagation characteristics of sixth-generation millimeter-wave signals at 28, 38, 73, and 142 GHz within tropical urban scenarios. All simulations are performed on the NYUSIM simulator with the standardized 3GPP TR 38.901 channel model. Simulations were performed under LOS and NLOS conditions with transmission distances ranging from 50 to 100 m. The analysis focused on path loss, received power, and RMS delay spread while incorporating local climate parameters representative of Banda Aceh, Indonesia. The results demonstrate that propagation performance degrades significantly as frequency increases. Path loss rises sharply with frequency and distance, with the most severe attenuation observed at 142 GHz under NLOS conditions. Consequently, received power decreases substantially at higher frequencies, indicating that reliable communication at frequencies above 70 GHz is highly dependent on clear LOS connectivity. Delay spread also increases with frequency and distance, reflecting more complex multipath dispersion in dense urban areas and suggesting potential challenges related to inter-symbol interference in wideband 6G systems. Overall, the findings show that lower mmWave frequencies (28–38 GHz) are more suitable for medium-range urban coverage, while higher frequencies (73–142 GHz) offer substantial capacity benefits but require advanced techniques such as high-gain directional antennas, adaptive beamforming, Reconfigurable Intelligent Surfaces (RIS), and dense small-cell deployment. The results provide one of the first propagation references for the 28–142 GHz range in tropical urban environments and offer essential insights for designing efficient and reliable 6G networks in Indonesia. Future work may include field measurement validation, modeling of dynamic blockage effects, analysis of beamforming gains, and integration of rain attenuation to further refine channel characterization for 6G deployments in tropical regions.

This study is fully based on system-level simulations using the NYUSIM simulator and the 3GPP TR 38.901 channel model. Therefore, the presented results are intended to provide preliminary insights for early-stage 6G network planning in tropical urban environments. The absence of field measurement data is acknowledged as a limitation of this work. Future studies will conduct measurement-based validation in real tropical urban settings to further assess the applicability and accuracy of the proposed climate-aware analysis framework.

Conflict of Interest

The authors declare no conflict of interest.

Author Contributions

Ami Lia Rizki conducted the research and wrote the draft of the paper; Yunida Yunida analyzed the propagation model; Syahrial Syahrial analyzed the results; Nasaruddin Nasaruddin investigated the research and reviewed the paper; all authors approved the final version.

Funding

This work is supported by the professorship research scheme, Universitas Syiah Kuala, under grant no. 391/UN11.L1/PG.01.03/14374-PTNBH/2025.

References

[1] M. Banafaa *et al*., "6G Mobile communication technology: Requirements, targets, applications, challenges, advantages, and opportunities," *Alexandria Eng. J*., vol. 64, pp. 245–274, 2023.

[2] W. Jiang *et al*., "Terahertz communications and sensing for 6G and beyond: A comprehensive review," *IEEE Communications Surveys and Tutorials*, vol. 26, no. 4, pp. 2326–2381, 2024.

[3] K. Bogens, "Main WRC-23 results with respect to terrestrial services," presented at ITU Regional Radiocommunication Seminar 2024 for the Americas (RRS 24-Americas), St. George's, Grenada, 2024.

[4] N. N. Maaruf, G. Hendrantoro, and A. Mauludiyanto, "Attenuation statistics for millimetre-wave links in tropical regions," in *Proc. 2023 IEEE International Symposium on Antennas and Propagation and USNC-URSI Radio Science Meeting*, 2023, pp. 403−404.

[5] I. Rahayu and A. Firdausi, "5G channel model for frequencies 28 GHz, 73 GHz and 4 GHz with influence of temperature in Bandung," *JTE J. Teknol. Elektro*., vol. 13, no. 2, pp. 24–99, 2022.

[6] B. Alfaresi, Z. Nawawi, R. F. Malik, K. Anwar, and L. O. Nur, "Humidity effect to 5G performances under Palembang channel model at 28 GHz," *Sinergi*, vol. 24, no. 1, pp. 49–56, Feb. 2020.

[7] Y. Xing and T. S. Rappaport, "Millimeter wave and terahertz urban microcell propagation measurements and models," *IEEE Communications Letters*, vol. 25, no. 12, pp. 3755–3759, Dec. 2021.

[8] T. S. Rappaport, Y. Xing, O. Kanhere, S. Ju, H. Nguyen, A. Madanayake, S. Mandal, A. Alkhateeb, and G. C. Trichopoulos, "Wireless communications and applications above 100 GHz: Opportunities and challenges for 6G and beyond," *IEEE Access*, vol. 7, pp. 78729–78757, 2019.

[9] A. Israr, Q. Yang, W. Li, and A. Y. Zomay, "Renewable energy powered sustainable 5G network infrastructure: Opportunities, challenges and perspectives," *Journal of Network and Computer Applications*, vol. 175, 102910, 2020.

[10] M. H. Alsharif, A. Jahid, R. Kannadasan, and M. K. Kim, "Unleashing the potential of Sixth Generation (6G) wireless

networks in smart energy grid management: A comprehensive review," *Energy Reports*, vol. 11, pp. 1376–1398, 2024.
[11] S. Ju and T. S. Rappaport, "Statistical channel model of wideband sub-THz radio propagation in indoor factories at 142 GHz: Toward 6G industrial wireless networks," *IEEE Transactions on Wireless Communications*, vol. 23, no. 4, pp. 2345–2360, 2024.
[12] C. Bian, W. Li, M. Wang, X. Wang, Y. Wei, and D. W. Zhou, "Path loss measurement of outdoor wireless channel in D-band," *Sensors*, vol. 22, no. 24, 9734, 2022.
[13] W. Jiang, B. Han, M. A. Habibi, and H. D. Schotten, "The road towards 6G: A comprehensive survey," *IEEE Open Journal of the Communications Society*, vol. 2, pp. 334–366, 2021.
[14] T. S. Rappaport, "The cellular concept—system design fundamentals," in *Wireless Communications: Principles and Practice*, Cambridge: Cambridge University Press, 2024, pp. 57–104.
[15] M. Theissen, L. Kern, T. Hartmann, and E. Clausen, "Use-case-oriented evaluation of wireless communication technologies for advanced underground mining operations," *Sensors*, vol. 23, no. 7, 3537, 2023.
[16] S. Sun, G. R. M. Cartney, and T. S. Rappaport, "A novel millimeter-wave channel simulator and applications for 5G wireless communications," in *Proc. IEEE Int. Conf. on Communications*, 2017, pp. 1–7.
[17] S. Cheerla, D. V. Ratnam, and H. S. Borra, "Neural network-based path loss model for cellular mobile networks at 800 and 1800 MHz bands," *International Journal of Electronics and Communications*, vol. 94, pp. 179–186, 2018.
[18] H. Poddar, S. Ju, D. Shakya, and T. S. Rappaport, "A tutorial on NYUSIM: Sub-terahertz and millimeter-wave channel simulator for 5G, 6G, and beyond," *IEEE Commun. Surv. Tutorials*, vol. 26, no. 2, pp. 824–857, 2024.
[19] Y. Wang, C. Wang, X. Liao, Y. Chen, Z. Yu, and G. Wang, "Millimeter wave and sub-THz channel measurements, models and comparisons in indoor industrial environment," in *Proc. 2024 IEEE 99th Vehicular Technology Conference*, Singapore, 2024, pp. 1–6.
[20] Badan pusat statistik kota banda aceh, banda aceh municipality in figures 2024, banda aceh, Indonesia. [Online]. Available: https://bandaacehkota.bps.go.id/en/statisticstable/3/V1ZSbFRUY3lTbFpEYTNsVWNGcDZjek53YkhsNFFUMDkjMw==/penduduk--laju-pertumbuhan-penduduk--distribusi-persentase-penduduk--kepadatan-penduduk--rasio-jenis-kelamin-penduduk-menurut-kecamatan-di-kota-banda-aceh--2021.html
[21] 3GPP. (2020). Study on channel model for frequencies from 0.5 to 100 GHz. ETSI TR 138.901 V16.1.0. [Online]. Available: https://www.etsi.org/deliver/etsi_tr/138900_138999/138901/16.01.00_60/tr_138901v160100p.pdf